Wireless Sensor Networking for "Hot" Applications: Effects of Temperature on Signal Strength, Data Collection and Localization

Kenneth Bannister, Gianni Giorgetti, Sandeep K.S. Gupta

IMPACT Lab, http://impact.asu.edu, Arizona State University

{Kenneth.Bannister, Gianni.Giorgetti, Sandeep.Gupta}@asu.edu

Abstract

We measured the attenuation of signal strength for Telos-class motes between 25 °C to 65 °C, with a maximum loss of 8 dB at 65 °C. A linear model for the combined reduction of the transmit power and receiver sensitivity is presented, which suggests significant impact on the transmission range and network services. Path loss and link budget analysis indicate a communication range reduction of up to 60%. Network simulations show that the maximum range reduction severely decreases average node connectivity and disrupts multihop data collection. When the received signal strength (RSS) values are used for localization without temperature compensation, ranging error increases by up to 150%. Moreover, Cramér-Rao Bound (CRB) analysis shows that even when the RSS values are compensated, localization errors increase as a result of reduced connectivity.

Categories and Subject Descriptors

C.4 [**Performance of Systems**]: Modeling techniques

General Terms

Design, Measurement, Performance, Reliability

Keywords

Temperature, Signal Strength, Variability, CC2420, Link Budget, Connectivity, Localization, Cramér-Rao Bound.

1 Introduction

Our research requires implementation of outdoor sensor networks in the Sonoran Desert of the southwestern United States, where daily summertime temperatures may vary from 25 °C to 45 °C, and temperatures in an exposed enclosure may reach 65 °C. In this harsh environment, we performed an RF site survey over several days using Telos-class motes. We observed a reduction in the signal strength that was strongest at the hottest time of day, resulting in a daily cycle as shown in Fig. 1. Similar variations were observed during experiments with WSNs for *smart containers* [6].
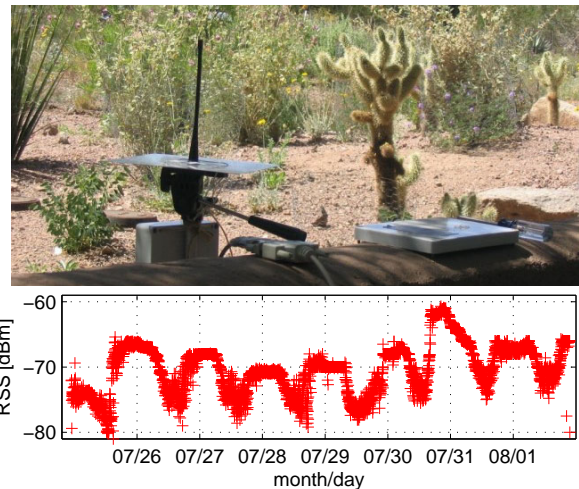
Figure 1. Deployment area and measured RSS.

To our knowledge, the WSN literature has not focused on the relationship between the link quality and the temperature. Lin *et al.* found a daily variation in the *Received Signal Strength* (RSS) of around 6 dB, but they did not explore the cause [7]. Thelen *et al.* mentioned an inverse relationship between the RSS and the temperature, but focused on humidity [17]. Sun and Cardell-Oliver found that a link may perform better during the day or at night, but suggested that humidity or noise was the cause [14]. Other studies have identified variations over shorter time periods without relating them to temperature [11, 20].

After the original observation of RSS in the site survey and additional qualitative experiments performed at various transmission levels using 433 MHz and 2.4 GHz sensor nodes, we attribute the periodicity of RSS measurements to the temperature variation during the day. Evidence that temperature decreases the efficiency of RF circuitry is found in [2, 18, 19], but no data that completely quantify the losses on mote hardware is available. The **aim** of our work is to characterize the effect of temperature on commercially-available sensor nodes, and to understand its implication on Wireless Sensor Network (WSN) deployments. Complementary to the focus in this paper, work in [16] studies networking strategies to minimize the impact of thermal energy generated by an environment-embedded (e.g. human) WSN.

In Sec. 2, we describe the experiments used to measure
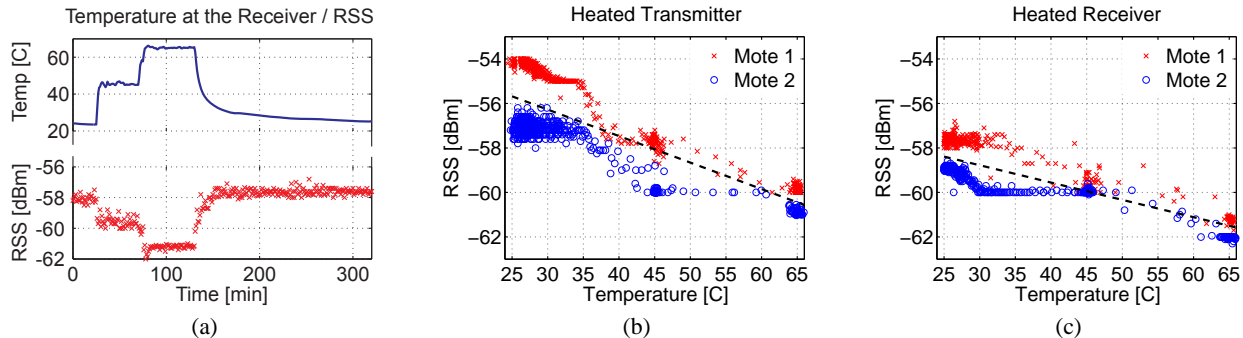
Figure 2. a) Example temperature profile at the receiver and RSS; b) RSS measurements when heating the transmitter, and c) when heating the receiver.

the RSS when sensor nodes using the TI CC2420 radio are exposed to a high temperature. We find that the RSS decreases linearly with the temperature. The resulting net decrease in RSS is about 8 dB for the transition from 25 °C to 65 °C. In Sec. 3 we show that this variation has a significant impact on the link budget of sensor nodes using low-power radios. In typical node configurations, the communication range can decrease by up to 60%, causing severe reduction in the network connectivity. In Sec. 4 and 5 we use the measured data in simulated scenarios to explore the effect of temperature on network services such as multi-hop data collection and localization. We show that an elevated ambient temperature can cause a large portion of the network to become disconnected and that the reduction in the RSS, if not compensated, can increase ranging errors by about 150%. Using the Cramér-Rao Bound (CRB), we show that even when the RSS values are compensated, localization errors increase due to the reduced connectivity.

The measurements are specifically obtained for the CC2420 transceiver that is used on some popular sensor nodes; however, the aim of our work is more general - we intend to bring awareness in the design and implementation of sensor networks with nodes subjected to temperature extremes. For example, in the FireBug sensor network used for wildfire monitoring, flame temperatures were reported to reach 95 °C in a grass fire [4]. Also, in WSN applications such as thermal monitoring in data centers, nodes can operate in temperature differences of more than 50 °C [15]. Using our data, a conservative design can be pursued to avoid loss of connectivity precisely when such critical applications require maximum reliability. We conclude the paper with lessons learned from our experiments and possible solutions to mitigate the temperature effects.

2 Thermal Effects on RSS

Our research uses the IEEE 802.15.4 compliant TI CC2420 radio [3] in a Tmote Sky wireless mote [8]. Both
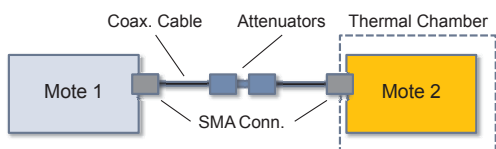
the CC2420 and Tmote tolerate an operating range of -40 °C to 85 °C. The CC2420 datasheet discusses the impact of temperature only in the context of frequency stability for the internal oscillator. However, the datasheet for the CC2400 does include graphs of the output power and receiver sensitivity over its operating temperature range, including [2]. Over our 40 °C range of interest, the output power decreases linearly at a rate of 0.75 dB per 10 °C and receiver sensitivity at 1 Mbps decreases at a rate of 1 dB per 10 °C for a combined reduction of 7 dB. In this section we measure the effect of temperature specifically for the CC2420 transceiver.

2.1 Experimental Setup

We performed lab experiments using two motes to characterize the effect of temperature on the signal strength. In order to eliminate the noise from any external sources and signal variability due to multi-path, the CC2420 radios on the motes were connected using a coaxial cable and a sequence of attenuators with nominal value of 60 dB (see Fig. 3).

The tests were performed by placing one of the two nodes in a thermal chamber and then raising the initial temperature to 45 °C and 65 °C before allowing the mote to cool down. As shown in Fig. 2(a), each level was maintained for at least 45 minutes to ensure thermal equilibrium between the air and the mote. The mote temperature was measured by the on-board Sensirion SHT11 sensor.

The power readings were collected by averaging the RSS over bursts of 10 packets transmitted every 40 sec, and sent at the maximum transmission power of 0 dBm. We performed a total of four trials, with each mote used as the transmitter and receiver, inside and outside the temperature chamber.

2.2 Results

The RSS readings collected at different temperatures for the transmitter and receiver are shown in Fig. 2(b,c). The graphs show clumps of readings at 25 °C, 45 °C, and 65 °C levels as described in the setup section above. The readings at 65 °C show 4-5 dB decrease in output power from the transmitter and 3 dB decrease in measured input power by the receiver, for approximately 8 dB decrease combined. We use a linear model to interpolate the data and quantify the power loss at the transmitter and receiver. The equation for the combined *Temperature Loss* (T_L) in dBm is:

$$T_L(T) = 0.1996(T - 25), \qquad (1)$$

Figure 3. Experimental Setup
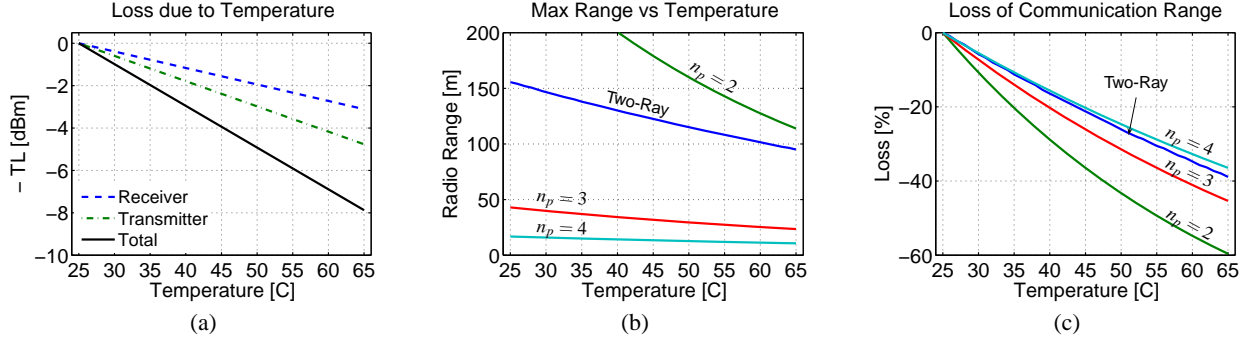
Figure 4. a) Contribution of the temperature losses by role; Absolute (b) and relative (c) reduction in communication range for log-distance and two-ray models (simulation parameters: $P_0 = -45\,\text{dBm}$, $d_0 = 1\,\text{m}$ and $P_s = -94\,\text{dBm}$).

where T is the temperature in the range $25 \leqslant T \leqslant 65$. The impact of T_L on the RSS is shown in Fig 4(a).

The losses measured when the transmitter is heated are similar, although slightly higher, to those reported by Yamashita *et al.* [19]. They used the CC2420 radio in a new mote and showed a linear decrease in the output power similar to the CC2400 datasheet, attributing the effect to a lack of thermal compensation in the CC2420 radio.

Additionally, we performed tests to measure the *Packet Error Rate* (PER) when the signal reaches values close to the transceiver *sensitivity*[1]. We controlled the power of the signal transmitted over the coaxial cable using a few additional attenuators. Once again we raised the mote temperature from 25 °C to 65 °C. We observed that regardless of the receiving mote's temperature, when the receiver's RSS reading fell below a particular value, for example -90 dBm, its PER began to increase. We therefore conclude that the losses observed when the receiver is heated (see Fig. 2a) are not due to a malfunction in the circuitry that measures the RSS, but they effectively correspond to a decreased ability of the radio to demodulate signals with low power. Our findings are consistent with the work of Wu *et al.* [18], where the temperature is shown to decrease the efficiency of the *Low Noise Amplifier*[2] (LNA) stage in a CMOS receiver.

3 Communication Range

Using (1), we can estimate the effect of temperature on the maximum communication range between two sensor nodes. We use the *Log-Distance Path Loss* model, which is commonly adopted for the link budget analysis in wireless communication. Under this model, the received power when the two nodes are at a distance d can be written as:

$$P_r(d) = P_r(0) - 10\,n_p \log(d/d_0), \qquad (2)$$

where $P_r(0)$ is the received power measured at the reference distance d_0, and n_p is the *path loss exponent*, a parameter that depends on the environment where communication occurs (typical values are between 2 and 4, [13]). In the absence of in-band interference, the probability of successfully receiving a radio message is high when $P_r(d)$ is above the radio sensitivity P_s, and then it rapidly decreases to zero as

---

[1] The IEEE 802.15.4 standard defines receiver sensitivity as the threshold power level to achieve less than 1% PER [1].

[2] The LNA is the circuit used to amplify the RF signal received from the antenna.

P_r falls below P_s. When the temperature affects communication, the additional loss decreases the received power and thus reduces the radio range. We define the maximum communication range $R_{\max}$ as the maximum value d that satisfies the inequality:

$$P_r(d) - T_L(T) \geqslant P_s. \qquad (3)$$

Given a pair of wireless devices, and fixed parameters for the path loss model, the value $R_{\max}$ is a function of the temperature. Fig. 4(a) reports $R_{\max}(T)$ for different values of the path loss exponent n_p. In addition to the log-distance path loss model, we also report the effect of temperature when the signal fades following the *two-ray* propagation model [12]. In a previous work we have experimentally verified that this model accurately describes the received power when nodes operate in uncluttered outdoor environments where reflections from the ground are the only significant source of multi-path [5]. In Fig. 4(b) we report the relative reduction in communication range as a function of the temperature increase. In all cases the maximum range significantly decreases, with reduction of up to 60% (log-distance) and 40% (two-ray) of the original value.

4 Multi-Hop Data Collection

Many outdoor applications such as environmental monitoring and precision agriculture require the monitoring of slowly varying signals such as the temperature and humidity over large areas. To keep the deployment and maintenance costs low, sensor nodes often are placed in a sparse configuration to minimize the number of units that cover the monitored area. However, since messages must be routed through a few radio links, communication is intrinsically more prone to failures, and accurate analysis of the link budget in the initial phase is critical to ensure reliable networking.

In this section we use simulation to show the effect of temperature on the network connectivity and common *source-to-sink* data collection applications. Consider the random topology shown in Fig. 5, where 49 nodes are deployed over a square region measuring approximately 250 m × 250 m, with Node 1 being collection sink. We obtain the network connectivity shown in Fig. 5 using the *log-normal shadowing* model [12] to simulate the path loss between pairs of nodes. Compared to the log-distance loss model used in Sec. 3, this model accounts for additional variability in the received power due to shadowing of the signal caused by obstructions in the deployment area. The received power
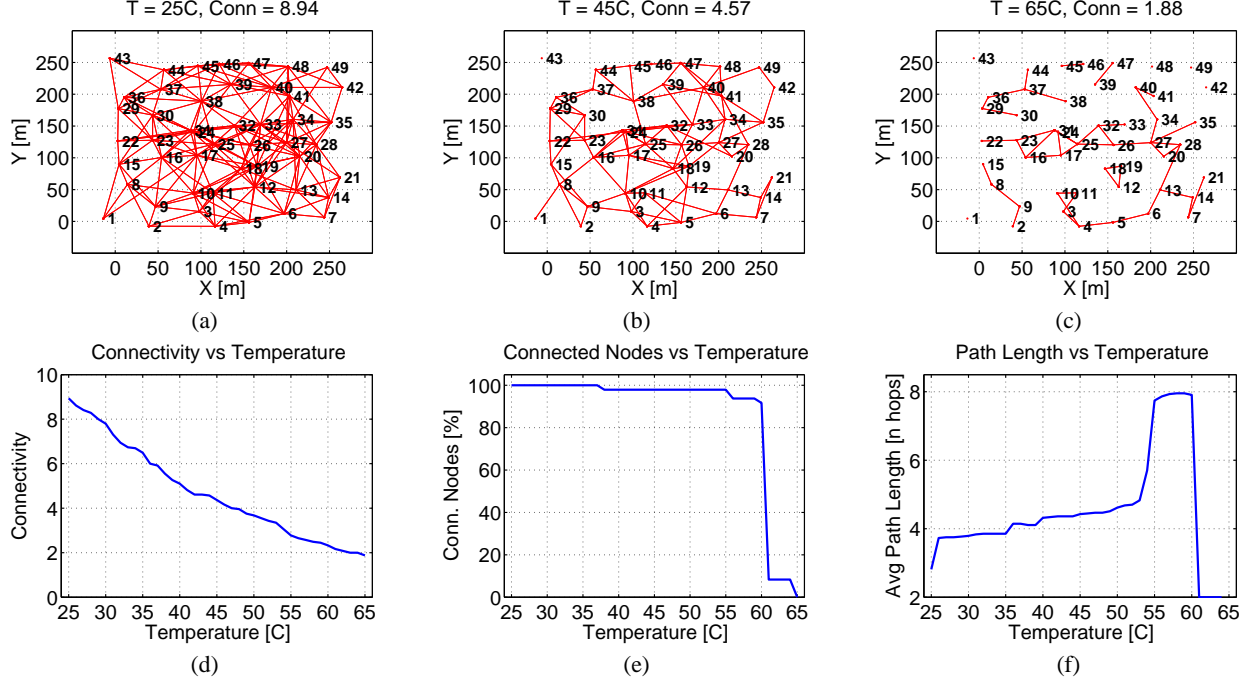
Figure 5. 7x7 node network simulation of network connectivity degradation with temperature. Node positions are generated using a *Noisy Grid* deployment model. Wireless parameters: $P_0 = -45\,\text{dBm}$, $d_0 = 1\,m$, $n_p = 2.5$, $\sigma_{\text{dB}} = 3\,\text{dBm}$, $Ps = -94\,\text{dBm}$. **a,b,c) Network topology at temperature = 25 °C, 45 °C and 65 °C; d,e,f) Effect of temperature on connectivity, % of nodes that can reach the sink, and average hop count to the sink, respectively.**

(in dBm) at distance d is modeled as a random variable:

$$P_{rs}(d) = P_r(d) + \Delta_S, \tag{4}$$

where $P_r(d)$ is the value defined in (2) and Δ_S is a zero-mean random variable with normal distribution $N(0, \sigma_{\text{dB}})$.

Fig. 5(a) shows the initial network state at 25 °C, where on average each node has around nine neighbors and 100% of nodes have a path to the sink. As the temperature rises to 65 °C, the reduction in communication range previously described steadily reduces the average node connectivity as shown in Fig. 5(b,c,d). Near the upper limit of the temperature range the percentage of nodes connected to the sink drops abruptly and the average path length increases dramatically as shown in Fig. 5(e,f). These changes occur typically when a *critical node* close to the sink loses connectivity to it. By this point many nodes have come to include that critical node in their path downstream to the sink, therefore when its link fails a large number of nodes become disconnected. Although the plots in Fig. 5 are relative to a specific topology, we have observed similar effects in many of our simulations.

5   Localization

In many WSN applications of practical interest, knowledge of the node positions is required to correctly evaluate the network results and to implement network services such as geographical routing and location-based query engines. Since use of a GPS receiver on every sensor node is not a cost-effective solution, alternative localization approaches have been actively researched over the past few years. Existing solutions can be grouped into *range-based* and *range-free* schemes depending on whether they use estimates of

ranges (e.g. distances) or they are based on proximity information (e.g. radio connectivity). Here we are interested in the case where both range and connectivity information are obtained by measuring the RSS between pairs of nodes. Although this is an appealing approach because no additional hardware is required, we show that temperature is a source of error that reduce the localization accuracy.

5.1   Ranging using Signal Strength

Consider the case where the received power follows the log-normal shadowing model described by (4). Given two nodes i and j at distance d_{ij}, the average RSS is given by $P_{ij} = Pr(d) + \delta_{ij}$, where δ_{ij} is a sample from the distribution $N(0, \sigma_{\text{dB}})$. The *Maximum Likelihood Estimate* (MLE) [9] for the distance d_{ij} is given by the following expression:

$$\hat{d}_{ij} = d_0 10^{(P_0 - P_{ij})/10 n_p}. \tag{5}$$

If the variance of the shadowing model were zero ($\delta_{ij} = 0, \forall i, j$), the expression above would produce the correct value of d_{ij}. In general, however, the presence of the term $\delta_{ij} \neq 0$ is a source of error in the distance estimates. When the temperature affects the radio communication, the losses at the transmitter and receiver produce additional variations in P_{ij} and increase the estimation error. Consequently, $P_{ij} = P_r(d_{ij}) + \delta_{ij} - T_L(T)$. Using (2) we derive an analytical expression for the ranging error:

$$e(d_{ij}, T) = \hat{d}_{ij} - d_{ij} = d_{ij} \left(10^{\frac{\delta_{ij} - T_L(T)}{10 n_p}} - 1 \right). \tag{6}$$

We see above that the combined error is proportional to the distance d_{ij} and it grows with the temperature. Fig. 6(a)

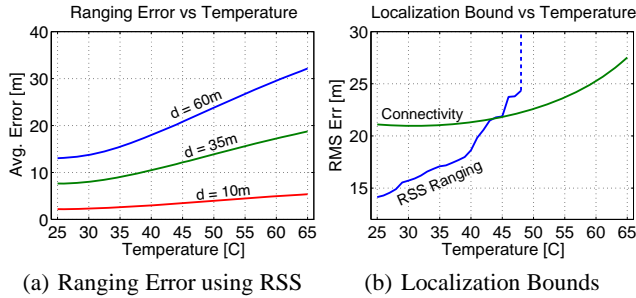(a) Ranging Error using RSS   (b) Localization Bounds

Figure 6. Ranging Error and Cramér–Rao Bound.

shows the average ranging error for three pairs of nodes placed 10, 35 and 65 meters apart, respectively, with $n_p = 3$, $\sigma_{dB} = 4$ dBm. We observe the error to increase by about 145% in the range between 25 °C and 65 °C. Although the effects on localization accuracy will vary depending on the localization scheme used, the effect of the temperature on the received power should be taken into account in order to avoid large errors in the position estimates.

5.2 Cramér–Rao Bound Analysis

If nodes have temperature sensors, the contribution of $T_L(T)$ can be removed from the average RSS in order to avoid the large ranging errors described in the previous section. However, even if the RSS is compensated, the reduction in the communication range will decrease the connectivity of the network and reduce the number of range estimates available to localize each node, resulting in increased localization error. We use the *Cramér–Rao Bound* (CRB) [9] to evaluate the effects on localization when the network connectivity decreases as a result of increased temperature. Fig. 6(b) shows the CRB when the range information obtained from RSS measurements are used to localize the topology in Fig. 5 using four nodes near the corners of the network as anchors.

As temperature reduces connectivity, the localization error rapidly increases, up to the point (~47 °C) where not enough range estimates are available to produce meaningful results. In the same figure we show the CRB computed using connectivity information [10]. The plot shows that while the accuracy initially is lower, temperature has less effect on a connectivity-based localization scheme. In fact, for RSS ranging no information is available from a pair of nodes unable to communicate, while a connectivity-based scheme is able to use "disconnected" nodes as information for localization. In general our simulations show that in sparse outdoor networks where nodes have a few neighbors, a connectivity based scheme may achieve better results, and it is more robust to decreases in connectivity due to temperature losses.

6 Conclusions

Our lab experiments confirmed the decrease in RSS that we originally observed outdoors when temperatures rose from 25 °C to 65 °C. We found the decrease to be linear and ranged up to 8 dB at 65 °C. We estimated the effect of the decrease on a node's communication range, and then used simulations to show its significant impact on network connectivity and services such as multi-hop data collection and localization. We make the following concluding observations:

- Our experiments used only the CC2420 radio on the Tmote Sky mote. Given the potential impact of temperature on the link budget of motes, we recommend similar investigations and characterization of temperature effects on the specific nodes used in a particular application.

- Temperature sensors should be included in each sensor node. Temperature awareness allows for compensation of the RSS variation and avoids large errors in localization.

- Sensor placement, enclosure and proper thermal insulation should be carefully evaluated to mitigate the effect of exposure to the sun or other heating sources.

- If the application tolerates communication delay, reliability may be improved by deferring communication to cooler time periods, e.g. during late night or early morning.

7 References

[1] IEEE Std 802.15.4-2006. http://standards.ieee.org/getieee802/download/802.15.4-2006.pdf.

[2] TI CC2400 datasheet. http://www.ti.com/lit/gpn/cc2400.

[3] TI CC2420 datasheet. http://www.ti.com/lit/gpn/cc2420.

[4] D. Doolin and N. Sitar. Wireless sensors for wildfire monitoring. *Proceedings of SPIE*, 5765:477, 2005.

[5] G. Giorgetti, A. Cidronali, S. Gupta, and G. Manes. Exploiting Low-Cost Directional Antennas in 2.4 GHz IEEE 802.15. 4 Wireless Sensor Networks. *The 37th European Microwave Conference, 2007, Munich, Germany*, 2007.

[6] S. J. Kim, G. Deng, S. K. Gupta, and M. Murphy-Hoye. Enhancing cargo container security during transportation: A mesh networking based approach. In *IEEE International Conference on Technologies for Homeland Security (HST)*, Waltham, MA, USA,, apr 2008.

[7] S. Lin *et al*. ATPC: adaptive transmission power control for wireless sensor networks. *The 4th international conference on Embedded networked sensor systems*, pages 223–236, 2006.

[8] Moteiv. Tmote Sky datasheet. http://www.sentilla.com/pdf/eol/tmote-sky-datasheet.pdf.

[9] N. Patwari *et al*. Relative location estimation in wireless sensor networks. *IEEE Transactions on Signal Processing*, 51(8):2137–2148, 2003.

[10] N. Patwari and A. Hero III. Using proximity and quantized RSS for sensor localization in wireless networks. *The 2nd ACM international conference on Wireless sensor networks and applications*, 2003.

[11] B. Raman *et al*. Implications of link range and (In) stability on sensor network architecture. *The 1st international workshop on Wireless network testbeds, experimental evaluation & characterization*, 2006.

[12] T. Rappaport. *Wireless Communications: Principles and Practice*. IEEE, 1996.

[13] K. Sohrabi *et al*. Near ground wideband channel measurement in 800-1000 MHz. *Vehicular Technology Conference, 1999 IEEE 49th*, 1, 1999.

[14] J. Sun and R. Cardell-Oliver. An experimental evaluation of temporal characteristics of communication links in outdoor sensor networks. In *Second ACM Workshop on Real-World Wireless Sensor Networks (REALWSN 2006)*.

[15] Q. Tang, S. K. S. Gupta, and G. Varsamopoulos. Thermal aware task scheduling for datacenters through minimizing heat recirculation. In *IEEE International Cluster Conference (Cluster)*, 2007.

[16] Q. Tang, N. Tummala, S. K. S. Gupta, and L. Schwiebert. Communication scheduling to minimize thermal effects of implanted biosensor networks in homogeneous tissue. *IEEE Transactions Biomedical Engineering*, jul 2005.

[17] J. Thelen *et al*. Radio wave propagation in potato fields. In *Proceedings of WNM workshop (co-located with WiOpt 2005)*, Riva del Garda, Italy, April 2005.

[18] Y. Wu *et al*. Temperature compensation design for a 2.4 GHz CMOS low noise amplifier. *Circuits and Systems, 2000. Proceedings. ISCAS 2000 Geneva. The 2000 IEEE International Symposium on*, 1, 2000.

[19] S. Yamashita *et al*. A 15x15 mm, 1uA, reliable sensor-net module: enabling application-specific nodes. *Information Processing in Sensor Networks, IPSN*, 2006.

[20] J. Zhao and R. Govindan. Understanding packet delivery performance in dense wireless sensor networks. *The first international conference on Embedded networked sensor systems*, pages 1–13, 2003.